Gene Co-Expression Network Analysis for Identifying Modules and Functionally Enriched Pathways in SCA2.

Lance T. Pflieger[1], Warunee Dansithong[2], Sharan Paul[2], Daniel Scoles[2], Karla P. Figueroa[2], Pratap Meera[3], Thomas S. Otis[3], Julio C. Facelli[1], Stefan M. Pulst[2]

[1]Department of Biomedical Informatics, University of Utah, Salt Lake City, Utah, 84112, USA

[2]Department of Neurology, University of Utah, Salt Lake City, Utah, 84112, USA

[3]Department of Neurobiology, University of California Los Angeles, Los Angeles, CA, USA

Corresponding author:

Stefan M. Pulst, MD, Dr. med.

Professor and Chair, Department of Neurology

Clinical Neurosciences Center, 175 North Medical Drive East, Salt Lake City, UT 84132

Phone: (801) 585-7575

Email: Stefan.pulst@hsc.utah.edu

Abstract

Spinocerebellar ataxia type 2 (SCA2) is an autosomal dominant neurodegenerative disease caused by a polyglutamine repeat expansion in the ATXN2 gene. We evaluated temporal gene profiles using RNA sequencing from mice with progressive ataxia, pcp2-ATXN2-Q127 and found early and progressive gene expression dysregulation. Weighted Gene Coexpression Network Analysis revealed four modules significantly correlated with disease status which included modules enriched with genes associated with GTPase mediated signaling, calcium signaling and cell death. Additional RNA sequencing of a knock-out mouse model, Atxn2$^{-/-}$, showed few overlapping differentially expressed genes when compared with the pcp2-ATXN2-Q127 model, suggesting that loss-of-function is not a significant part of disease pathology.

Introduction

SCA2 is among the neurodegenerative polyglutamine (polyQ) diseases as it is caused by a CAG repeat expansion in the ATXN2 gene giving rise to an expanded polyQ domain(1). Other polyQ diseases include SCA1, SCA3, SCA7, SCA17, Huntington's disease, spinal bulbar muscular dystrophy and dentatorubral-pallidoluysian atrophy. SCA2 is an autosomal dominant disorder characterized by symptoms resulting from neurodegeneration of the cerebellum and selective loss in the brainstem and spinal cord. Symptoms are characterized by progressive loss of coordination, unstable gait, nystagmus and dysarthria. As is common with other SCAs, a prominent feature of disease progression is the loss of Purkinje neurons(2).

Multiple transgenic mouse models have been generated to elucidate the role of ATXN2 in SCA2(3, 4). The pcp2-ATXN2-Q127 mouse model contains 127 CAG repeats in the full-length ATXN2 gene under the control of the Purkinje cell targeted pcp2 promoter. The model showed early onset deficits in motor function as early as 8 weeks. These changes were preceded by electrophysiological changes at 6 weeks and gene expression changes at 4 weeks. The observed gene expression changes were identified by relying on previously established PC marker genes, genes known to be specifically expressed in the PCs such as *Calb1* and *Pcp2*. An Atxn2-CAG42 knock-in mouse model has also been generated(5). In contrast to the transgenic models, this model did not show show overt ataxic behavior, with the exception of homozygous knock-in animals at 18 weeks, which were associated with Pabpc1 deficiency. Microarray analysis of the symptomatic Atxn2-CAG42 knock-in revealed few changes in mRNA levels when compared to wild-type including no significant changes to the PC marker *Calb1*. Additionally, multiple knock-out mouse lines have also been reported and characterized(6, 7). These loss-of-function models have been associated with obesity, dyslipidemia and insulin resistance.

Generally, mouse models are used to characterize behavior over the progression of the disease and identify accompanying pathological features. Increasingly, models are being utilized to study disease progression using a system biology approach(8, 9). Such approaches seek to identify functional pathways involved in disease progression, potentially providing new therapeutic targets.

To gain a better understanding of SCA2 disease progression, we analyzed RNA-sequencing data from cerebella of Pcp2-ATXN2-Q127 at three distinct time points which

represented cerebellar developmental, pre-pathological and early disease development. Using weighted gene co-expression network analysis (WGNCA), we identified multiple modules associated with disease progression including a module enriched for Purkinje cell transcripts and a module indicative of cell death. Additionally, we provide a comparison with Atxn2$^{-/-}$ mice showing little overlap between the two models.

Results

Temporal differential expression analysis of Pcp2-ATXN2-Q127 mice

SCA2 mice are characterized by progressive worsening of molecular, motor and physiological phenotypes, with the earliest biochemical changes detected at 4 weeks of age, as described in Hansen et al (3). To further characterize the SCA2 mouse molecular phenotype and its progression, we analyzed gene expression by RNA sequencing of cerebellar tissues from Pcp2-ATXN2-Q127 (ATXN2-Q127) and age matched wild-type (WT) mice. Cerebellar tissue was collected at 3 time points: an early developmental stage (1 day), a pre-pathological stage (3 weeks) and a stage where electrophysiological changes are detectable (6 weeks). RNA libraries were generated from multiple biological replicates from each group and subsequently sequenced on an Illumina HiSeq platform (see methods). We identified 146, 458 and 445 differentially expressed genes (DEGs) relative to WT at the day 1, week 3 and week 6 time points, respectively (fold change ≥ 1.5 or ≤ -1.5, p-value <0.01). A larger number of genes had greater fold changes in expression occurring at later time points (Supplementary 1). Of the significant DEGs, few were shared across all time points, with the greatest percentage of shared genes occurring between weeks 3 and 6 (Fig. 1).

Enrichment Analysis

Gene ontology (GO) analysis using DAVID showed that the shared genes between weeks 3 and 6 were strongly enriched for annotations in biological process (BP), molecular functions (MF) and cellular components (CC) related to calcium signaling and ATPase activity(10, 11). In contrast to the genes shared between day 1 and week 3, the shared genes between week 3 and week 6 showed strong enrichment for cell growth and regulation. Day 1 and week 6 shared genes showed only enrichment in BP terms related to cell growth (Supplemental Enrichment). Globally, stronger changes in down-regulated genes were seen compared to up-regulated genes at each time point (Fig. 1). GO analysis of the significantly down- and up- regulated genes at each time point showed that terms related to calcium ion binding were significantly enriched for the downregulated genes across all time points, with each time point increasing in significance (Supplementary Table 2). At week 3, BP terms related to developmental processes were significantly enriched for downregulated genes. Terms related to apoptosis became significantly enriched for upregulated genes in week 6, whereas downregulated genes were strongly enriched for terms related to ion transport, Purkinje cell development and cell signaling.

Purkinje cell specific genes are down-regulated in cerebella of SCA2 mice

Top-ranked downregulated genes at week 6 included multiple previously-identified Purkinje cell markers such as *Trpc3*, *Garnl3*, *Doc2b* and *Dner* (ranked 4^{th}, 10^{th}, 18^{th}, and 22^{nd} respectively). Of the list of known annotated Purkinje cell marker genes provided by Rong, Wang and Morgan(12), 7/30 were down-regulated at week 3, increasing to 23/30 by week 6. No markers were differentially expressed at day 1 (Supplementary

Purkinje Cell List). Early down-regulated Purkinje cell markers included *Atp2a3, Cacna1g, Dner, Doc2b, Fgf7, Garnl3* and *Pcp2*.

Upregulated genes

Across the time points, the number of down-regulated DEGS far exceeded the number of up-regulated DEGs. Specifically at the 3 and 6 week time points, only 97 out of 454 and 130 out of 434 were up-regulated, respectively. Only *Casp3, Adcyap1, Coch, Pappa* and *Mbl2* were significantly up-regulated at 3 and 6 weeks with the cut-offs used for this analysis. Of note, both Casp3 and Adcyap1 are key in cellular response to stress. Also, *Mbl2* was the top up-regulated gene at week 3 and the second most up-regulated gene at week 6. The *Mbl2* gene encodes for mannose binding lectin which has been shown to bind amyloid β peptides(13).

Weighted gene co-expression network analysis

To gain a better understanding of the transcriptomic changes at a systems level, we used weighted gene co-expression network analysis (WGCNA)(14, 15). WGCNA uses transcriptomic data to identify biologically meaningful gene clusters known as co-expression modules. Co-expression modules can facilitate the finding of hub genes that are key drivers of module function and may correspond to biological pathways(16).

Data from the week 3 and week 6 time points were used in the WGCNA analysis. The day 1 time point was not used as the large differences in developmental gene expression between day 1 and week 3 created physiologically implausible modules. The top-most variable genes (see Methods) were used as WGCNA input. Topological overlap was used for clustering, resulting in 16 modules, as can be seen from the color-

band underneath the cluster tree (Fig. 2A). Modules were arbitrarily assigned colors with sizes ranging from 90 (darkgrey) to grey (1604). The grey module consisted of genes that do not group into any specific module.

Identification of modules associated with mutant polyQ-expanded ATXN2

To identify relevant modules associated with SCA2 pathology, we assessed the relationship between ATXN2 mutation status and the module eigengene, a weighted summary of the gene expression module(17). We identified four modules, black (r = 0.48, *P* = 6.7e-3), darkgrey (r = 0.67, *P* = 1.5e-7), darkred (r =0.79, *P* = 2.5e-11) and midnightblue (r = 0.89, *P* = 2.2e-16) that showed significant enrichment for genes with differential expression between ATXN2-Q127 and WT mice (Fig. 2, Supplementary Fig. 2). Fig. 3 visualizes the connectivity patterns and hub genes (Table 1) of the relevant modules. Hub genes are identified per module using WGCNA's intramodular connectivity score, a measure of the cumulative connectivity a gene has with all other genes in a given module.

The black module consisted of 376 genes loosely correlated with SCA2 pathology. GO analysis revealed that the module was enriched with genes identified as regulators of small GTPase mediated signal transduction (*P* = 1.8e-3), mRNA transport (*P* = 5.2e-3) and phosphorylation (*P* = 5.4e-3). Kegg pathway analysis showed this module to be enriched for axon guidance (*P* = 4.8e-3).

The dark grey module contained 90 genes including multiple Purkinje cell markers (*Calb1, Car8, Casq2, Fgf7, Gng13, Kitl, Pcp4, Stk17b, Sycp1,* and *Trpc3*). GO analysis revealed enrichment of terms related to ER-nuclear signaling (*P* = 3.5e-3), regulation of

apoptosis (*P* = 1.3e-2), and positive regulation of cell differentiation (*P* = 2.4e-2). Interestingly, many of the PC marker genes are highly connected hub genes, such as *Calb1*, *Stk17b* and *Pcp4*.

The dark red module had 107 genes including multiple PC markers (*Garnl3, Homer3, Icmt, Itpka, Pcp2* and *Slc1a6*). GO analysis revealed genes enriched with terms related to regulation of small GTPase mediated signal transduction (*P* = 5.2e-5) and intracellular signaling cascade (*P* = 4.2e-4).

The midnight blue module had the highest correlation with disease status as determined by the gene significance measure. It contained 159 genes, including PC markers (*Atp2a3, Cacna1g, Dner, Doc2b, Grid2, Inpp5a* and *Itpr1*). Interesting enriched GO terms included metal ion transport (*P* = 5.6e-5), cerebellar PC layer development (*P* = 4.1e-3) and synaptic transmission (*P* = 8.2e-3). Kegg pathway analysis revealed the module to be related to long-term depression (*P* = 2.5e-4), phosphatidylinositol signaling system (*P* = 2.9e-3) and the calcium signaling pathway (*P* = 392e-3), all pathways well known to be crucial for PC functioning.

Validation of key DEGs

We validated the relative expression levels of hub genes from the co-expression network analysis using quantitative RT-PCR (Fig. 4). We found that 100% of the 12 genes analyzed were significantly differentially expressed in the cerebella of ATXN2-Q127 mice compared to WT littermates. Validated hub genes include *Smarca4, Rusc2* from the black module, *Gabbr2* from the midnightblue module, *Cep76, Calb1* and *PCP4*

from the dark grey module and *Gabbr1, Fam21, DGKZ* and Aldoc from the dark red module. *Casp3* was also validated as significantly up-regulated at week 3.

MicroRNAs

Several links between microRNA (miRNA) regulation and polyglutamine repeat associated ataxias are known(18, 19). To identify alterations in miRNA expression associated with SCA2, cerebellar samples from mice 3 weeks of age and age-matched controls were used to isolate total RNAs. Small RNA libraries were generated from four biological replicates from each group and subsequently sequenced on an Illumina HiSeq platform (see methods). An average of 29.6 million reads was generated from the eight libraries, ranging from 23.1 to 36.3 million. Out of the 297 million reads, 135 were able to be mapped to the mouse genome (mm10). Differential expression analysis was performed and identified 16 annotated miRNA and four snoRNAs with a fold change greater than 1.5 ($P < 0.01$). With the exception of the snoRNA *Gm24895*, all transcripts were down-regulated in cerebella of ATXN2-Q127 mice (Table 2).

***Atxn2*$^{-/-}$ mice have few cerebellar DEGs**

Atxn2 deficient mice (*Atxn2*$^{-/-}$) are viable and have only slight phenotypic changes compared to wildtype littermates(6). However, it is unknown if the non-essential role of ataxin-2 in mice is due to the presence of orthologs or redundant mechanisms. To further investigate the role of *Atxn2,* we analyzed gene expression using RNA sequencing of cerebellar tissues of *Atxn2*$^{-/-}$ and age matched wild-type mice. Cerebella from 1 day and 60 day old wild-type, heterozygous and Atxn2$^{-/-}$ mice were collected,

each with multiple biological replicates. RNA libraries were generated from each group and subsequently sequenced on an Illumina HiSeq platform (see methods).

We identified 46 differentially expressed cerebellar genes (fold change ≥ 1.5 or ≤ -1.5, p-value <0.01) between *Atxn2*$^{-/-}$ and age matched wild-type mice at 1 day and 11 genes at 60 days (Supplementary X KO expression). Only two genes were differentially expressed at both time points (*Ubc*, *Gm8730*). Of the DEGs, 16 were up-regulated and 30 were down-regulated at 1 day and five were up-regulated and six down-regulated at 60 days.

No pathway overlap between *Atxn2*$^{-/-}$ and ATXN2-Q127 mice

To find overlapping pathways between *Atxn2*$^{-/-}$- and Pcp2-ATXN2[Q127] mice, we compared the overlap among DEG lists at each time point (Fig. 5). The remarkably few number of significantly changed cerebellar genes between *Atxn2*$^{-/-}$ and wild-type mice, in contrast to the large number of differentially expressed genes between ATXN2-Q127and wild-type mice is consistent with the gain-of-function model for the expanded polyglutamate disease.

Purkinje cell firing rates in the acute cerebellar slice in Atxn2$^{-/-}$ mice

After considering the lack of phenotypic and transcriptomic similarities between the Atxn2$^{-/-}$ and ATXN2-Q127 mice, we elected to investigate electrophysiological behavior of Atxn2$^{-/-}$ Purkinje cells. This allowed the examination of the effect of *Atxn2* knock-out on the neurophysiological phenotype using methods established by Hansen et al (3). We utilized noninvasive extracellular recording techniques to measure the intrinsic PC firing rate in cerebellar slices at ages 4, 12 and 24 weeks. The average mean firing

frequency over populations of PCs is shown in Fig. 6 using population distributions. To generate the distribution, the mean firing frequency was calculated over 2 min time periods for multiple PCs and plotted for each age. A one second snap-shot of the firing frequency at each age is shown in Fig. 6. The mean firing frequency is indicated for each age. In contrast to Pcp2-ATXN2[Q127] animals that show a progressive slowing of PC firing beginning at age 8 weeks, the firing frequency remained normal in *Atxn2*$^{-/-}$ mice.

Discussion

We performed RNA sequencing analysis in an SCA2 mouse model that targets expression of the mutant polyQ- expanded ATXN2 to PCs. Our use of multiple time points and differential expression analysis showed that genes were differentially expressed as early as 1 day, with an increasing number of genes and greater fold-changes at later time points. Furthermore, 16 miRNAs and 4 snoRNAs were differentially expressed as early as 3 weeks. These observations were all made with stringent cut-offs for fold-change and significance levels for multiple comparisons.

Subsequent analysis of the DEGs using WGCNA allowed us to identify four gene modules related to disease progression. Investigation of these modules revealed novel hub genes and pathways that are likely biologically relevant to disease status.

Comparison of the ATXN2-Q127 and Atxn2$^{-/-}$ expression datasets showed negligible overlap. Additionally, PC firing in the acute slice in the knock-out model was unchanged in contrast to the transgenic model in which the intrinsic firing frequency becomes progressively slower with age (Hansen paper). Taken together, these data give insight

into the SCA2 disease progression, are consistent with a gain-of-toxic-function associated with *ATXN2* mutation. Furthermore these data support ongoing research on the development of SCA2 therapeutics that lower *ATXN2* expression targeting both wt and mt alleles.

Transcriptomic comparison

Several studies have examined changes in mRNA steady-state levels in SCA mouse models. Most of these used expression arrays (refs), but a recent analysis of an SCA1 model employed RNA-seq and analysis by WGCNA(20). Transcription dysregulation commonly seen in polyglutamine disorders and comparison of gene expression among the polyglutamine diseases has revealed many commonly occurring changes(21, 22). We also find similarities between published polyglutamine expression profiles and our SCA2 profile. Everet et al. determined gene expression changes in SCA3 cell models(23). While not a perfect comparison, non-cerebellar genes and pathways were revealed. Of note, both studies demonstrated changes to extra-cellular related molecules such as *TIMP1* and *TIMP2*. Our full differential expression analysis, discussed below, showed large changes in genes associated with the ECM occurring as early as day 1. This overlap suggests disruption of processes involved with the ECM such as cellular adhesion. Similarly we find high overlap with laser-capture PC expression profiles from Huntington's and SCA7 mice(22). Unsurprisingly, many PC markers are common to both sets including *Calb1, Pcp4, Itpr1, Slc1a6* and *PCP2*. Other overlapping genes that are also differentially expressed in SCA1, SCA3, SCA7 or DRPLA include *Grid2*, *Aloc, Fam107b, Dagla, Rgs8, Nptx1* and *Plcb3*. Furthermore, many movement disorders are associated with the dysfunction of PGC-1α, a master

regulator of mitochondrial biogenesis. While not a polyglutamine expansion disease, Lucas et al. showed evidence of PC loss in a PGC-1α deficient mouse model(24). No overlap was found between the PGC-1α dependent transcripts, suggesting different roles in neurodegeneration.

Comparison to similar studies on SCA1

Although the disease models mentioned above provide an insight into shared transcriptome changes in neurodegeneration, the recently published SCA1 dataset is most relevant to our study(20). Ingram et al. used RNA sequencing of SCA1 mouse cerebellar tissues and subsequent WGCNA analysis to identify two modules related to SCA1 pathology, Magenta and Lt. Yellow. We found no significant overlap with the SCA1 Lt. Yellow module but three of our SCA2 related modules (dark grey, dark red and midnight blue) had significant overlap with the SCA1 magenta module. There were 33 genes of the SCA1 magenta module that overlapped with the SCA2 dark grey module ($p<0.001$), 34 with the dark red module ($p<0.001$) and 51 with the midnight blue module ($p<0.001$) (Supplemental SCA1_SCA2). Using the top 100 connected genes of the SCA1 magenta module, we found that 92 are also in the overlapping SCA2 modules including multiple PC marker genes. Furthermore, we found that genes identified as highly interconnected or hub genes in the SCA1 magenta module were also found to be highly interconnected in the SCA2 modules including *Fam21*, *Gabbr1* and *Homer 3* from the magenta/dark red module overlap and *Rgs8* and *Lcmt* from the magenta/midnight tblue overlap. To identify why one SCA1 module had significant overlap with three SCA2 modules, we re-analyzed our SCA2 data with increased merge cut-height and soft-threshold power (see methods). The re-analysis resulted in a module (purple) with

overlap of 210 genes (Supplementary SCA1_SCA2), suggesting module differences are a result of WGCNA parameters and filtering choices. The SCA1 study also revealed a likely PC protective gene, *Cck*. We also detected differential expression of this gene and the associated receptors (*Cckar*, *Cckbr*) in our SCA2 model.

Temporal mRNA changes

Changes in expression as early as day 1

The use of multiple time points allowed us to identify early changes and trends associated with disease pathology. We observed that presence of an expanded ATXN2 polyQ repeat resulted in altered gene expression as early as day 1. While a smaller number of genes were altered compared to the later time points, a portion of these genes were associated with terms suggesting a disruption of normal development. For instance, up-regulated genes are associated with histone acetylation and chromatin remodeling while down-regulated genes are associated with cell adhesion and extracellular matrix terms. It is unknown whether the disruption caused early morphological differences or delayed development. Many of the genes associated with cell growth and development, however, remained downregulated in mice 3 weeks of age. Of note, detailed morphology and physiology of transgenic cerebella did not show any changes prior to 6 weeks of age.

Calcium signaling changes start early

Irregularities in calcium signaling have been associated with multiple neurodegenerative diseases including SCA2 (SCA2-Lui, SCA3-Chen, SCA6-Watase). At day 1, we noted a downregulation in 16 genes associated with calcium ion binding. This number increased

to 31 genes by week 3 and included a downregulation of multiple genes in the calcium signaling pathway (*Atp2b2, Atp2a3, Adra1a, Cacna1g, Camk2a, Itpr3, Nos1, Oxtr* and *Plcb3*).

Apoptosis by week 6

Examining the widespread expression changes occurring by week six, we noticed a subset of upregulated genes. These genes were largely associated with regulation of apoptosis including *Casp3, Bid, HRK, Btg2, Hspa1, Hgf, Ntf3* and *Timp1*. With the accompanying down-regulation of many PC markers, we suggest PC degeneration begins to occur as early as 6 weeks, after notable dysregulation of genes associated with calcium signally changes.

Knock-out changes

Previous studies demonstrated that SCA2 pathogenesis was likely caused by gain-of-toxic-function due to the expanded polyQ repeat in ATXN2 (REFS). However, the extent to which a loss of *Atxn2* function contributed to pathogenesis was unknown. Several other types of ataxias have revealed that the loss of the involved proteins does not lead to neurodegeneration(25, 26). Yet, the deletion of *ATXN1* enhanced SCA1 pathogenesis(27).

Disease progression by 6 weeks causes large transcriptional changes in the ATXN2-Q127 mouse with over 400 genes differentially expressed when compared with WT. In contrast, relatively small changes were seen in the knock-out mouse model with only 11 genes differentially expressed when compared with WT at an age when the transgenic

mouse shows significant disease. Comparing the overlap between Atxn2$^{-/-}$ and ATXN2-Q127 transcriptomes at the later time point shows five out of the ten Atxn2$^{-/-}$ DEGs were shared with Pcp2-ATXN2Q[Q127] While this overlap is significant, the small number of expression changes argues strongly that loss-of-function is not a significant part of disease pathology. In addition, the day 1 comparison had only three overlapping genes. The lack of overlap is consistent with a gain-of-function in SCA2 mice. In contrast to transcriptome analyses of SCA1 mice indicating gain-of-function with partial loss of function(27), we could find little evidence for partial loss of function in our SCA2 mice. These conclusions based on transcriptome analyses were also supported by the lack of PC firing changes in the acute cerebellar slice in knockout animals. Whereas Pcp-ATXN2[Q127] animals show a progressive decline in spontaneous PC firing beginning at 8 weeks of age, PCs in *Atxn2*$^{-/-}$ mice retained a normal firing rate even as late as 24 weeks of age.

WGCNA

WGCNA is a technique used to identify highly correlated gene modules which can be related to external factors such as disease status. We applied this unsupervised, hypothesis-free method to construct co-expression networks in polyQ expanded SCA2, revealing pathologically relevant gene modules. This approach has been used successfully in a number of neurodegenerative diseases, helping to elucidate disease pathways and associated genes (28–31). In SCA2, little is known about gene expression changes that precursor electrophysiological and motor phenotype in SCA2 disease progression. The use of a hypothesis-free approach allowed us to increase the

current knowledge of expanded polyglutamine pathology in SCA2 and provide new avenues for future research.

Modules

We identified four modules correlated with disease status that can be summed into known pathological associations with SCA2 including GTPase mediated signaling, calcium signaling and cell death. Interestingly, the largest of these, Black, did not contain any PC markers. It contained multiple genes associated with regulation of small GTPase signal transduction (*Plekhg3, Smap2, Bcr, Sgsm1, Tbc1d9, Tiam1, Prex1, Trio, Agap1, Tbc1d22b, Rapgef1, Arhgef11*), synaptogenesis (*App, Nrxn2, Dlg4*) and axon guidance (*Ablim1, Ablim2, Sema4g, Unc5a, Plxnb3, Sema4b, Sema4d, Sema3a*). This module provides an insight into the dysregulation of neurodegenerative cell morphology. The darkred module is similarly associated with regulation of GTPase mediated signal transduction (*Garnl3, Agfg2, Rapgef6, Iqgap2, Dgkz, Icmt, Cyth3, Psd2*). However, it was not found to be enriched for any other GO term or KEGG pathways. The dark grey module is enriched for genes associated with programmed cell death (*Trp53, Stil, Clu, Stk17b, Eif2ak3, Kitl, Acvr1c*). It provides additional information on the early apoptotic cycle in the cerebellum. Of note, pathway analysis of this module showed an overlap with pathways associated with cancer due to the genes *TRP53, CCND1, FGF7,* and *ACVR1C*. Also, three of the top four genes ranked by intermodular connectivity, or hub genes, are known PC markers *Calb1, Stk17b* and *Pcp4* providing evidence that further analysis of this module may provide novel PC markers. Lastly, the midnight blue module is significantly associated with calcium signaling (*Atp2b2, Plcb3, Atp2a2, Atp2a3,*

Cacna1g, Grm1, Itpr1) and PC layer development (*Atp2b2, Lhx5, Klhl1)*. Further investigation into this module could elucidate early transcriptional changes in PCs. This module also had overlap with an Alzheimer's disease pathways. Complete GO term categories and associated genes can be found in the supplemental material (STXX).

microRNAs in Neuro

Finally, the identification of early transcriptional changes in miRNAs presents opportunities for further investigation into disease pathogenesis. MiRNAs and snoRNAs have important roles in many neurodegenerative diseases, including Parkinson's, amyotrophic later sclerosis (ALS) and Alzheimer's disease (19, 32). Our results at 3 weeks of age show changes in 16 annotated miRNAs and 4 snoRNAs including *Snord115* which has a decrease of over eight-fold when compared with WT.Since *Snord115* is a gene cluster containing at least 130 copies in mouse, it is likely that the difference in expression is due to sequencing alignment error. However, previous studies have demonstrated increased expression of Snord115 correlate with increased calcium ion response to GPCR mediated signaling (Autism-nakatani).Considering the notable changes to genes associated with calcium signally at 3 weeks of age, it is plausibly that the large decrease of this snoRNA in ATXN2-Q127 is in response to an early imbalance in calcium signaling. Further research is needed.

Materials and Methods

RNA Sequencing and analysis

Total RNA was isolated using miRNeasy Mini Kit (Qiagen Inc., USA) according to the manufacturer's protocol. RNA quality was determined using the Bioanalyzer2100 Pico

Chip (Agilent). Samples with an RNA integrity number (RIN) >8 were used for library preparation using Illumina TrueSeq Stranded Total RNA Sample Prep with Ribo-Zero rRNA Removal Kit for mouse. Single-end 50-bp reads were generated on a Hiseq 2000 sequencing machine at the University of Utah Microarray and Genomic Analysis Shared Resource using Illumina Version 4 flow cells. Reads were then aligned to the mouse reference genome (mm10) by Novoalign (http://www.novocraft.com). Quality of RNA sequencing was good with an average of twenty two million reads for Pcp2-ATXN2[Q127]. Ninety eight percent of the reads were aligned to the reference mouse genome. After read alignment, differentially expressed genes were identified using the DRDS application (version 1.3.0) in the USeq software package (http://useq.sourceforge.net/).

Co-expression network

RNA-seq data from the week 3 and week 6 timepoints were first filtered by FPKM (≥ 1.0 in 90% of samples) to reduce noise. Further filtering on the coefficient of variation (≥ 0.15) was used to get the most variable genes, resulting in 7694 transcripts. The unsigned WGCNA was conducted as previously described using the R package WGCNA (PMID 19114008). Briefly, a similarity matrix was constructed using the Pearson correlation coefficients created between the FPKM normalized expression levels of the input transcripts. By raising the absolute value of the Pearson correlation coefficients to a power of 14, we were able to get a scale-free topology index above 0.9, achieving a network with few, large correlations at the expense of lowly correlated transcripts. This allows for the fewer, highly connected and biologically relevant hub genes. An adjacency network was then created using topological overlap measure

(TOM), a measure of neighborhood connectivity. To create modules, the adjacency network was converted into a dissimilarity measure (1 – TOM) and clustered using flashClust, a hierarchical clustering function. Cluster branches were cut to identify modules. Module size was set to a minimum of 50 transcripts and modules with a 10% similarity were merged using dynamic tree cutting, resulting in 16 modules. To identify significant modules, Gene Significance (GS) was calculated as the absolute value of the correlation between gene expression and transgenic status. Overall significance for each module was calculated by averaging all GS within each module. Statistical significance was determined using the correlation t-test p-value.

RNA expression analyses by quantitative RT-PCR

Mice were deeply anesthetized with isoflurane. Mouse cerebella were removed and immediately submerged in liquid nitrogen. Tissues were kept at −80°C until the time of processing. Total RNA was extracted from mouse cerebella using the RNeasyMini Kit (Qiagen Inc., USA) according to the manufacturer's protocol. DNAse I treated RNAs were used to synthesize cDNAs using the ProtoScript cDNA First Strand cDNA Synthesis Kit (New England Biolabs Inc., USA). Quantitative RT-PCR was performed in Bio-Rad CFX96 (Bio-Rad Inc., USA) with the Power SYBR Green PCR Master Mix (Applied Biosystems Inc, USA). PCR reaction mixtures contained SYBR Green PCR Master Mix and 0.5 pmol primers and PCR amplification was carried out for 45 cycles: denaturation at 95°C for 10 sec, annealing at 60°C for 10 sec and extension at 72°C for 40 sec. The threshold cycle for each sample was chosen from the linear range and converted to a starting quantity by interpolation from a standard curve run on the same plate for each set of primers. All gene expression levels were normalized to the Actin

mRNA levels. Primer pairs designed for qRT-PCR are given as forward and reverse, respectively, and listed in supplementary table. (Sharan will send)

Functional Enrichment Analysis

Gene Ontology and pathway-enrichment analysis (KEGG) was conducted using the functional annotation tool DAVID (https://david.ncifcrf.gov/). Enriched ontological terms and pathways with a P value less than 0.05 were selected.

MircoRNA

Cerebellar extract from mice 3 weeks of age with 4 biological replicates and age-matches WT controls were used for microRNA library construction. The construction of Small RNA sequencing libraries was performed using the Illumina TruSeq Small RNA Sample Prep Kit (RS-200-0012, RS-200-0024). Most mature miRNAs have a 5'-phosphate and a 3'-hydroxyl as a result of the cellular pathway that creates them. The adapters are designed to specifically ligate to RNA molecules containing these terminal modifications. Briefly, total RNA (1 ug) was denatured and 3' and 5' RNA adapters were sequentially ligated to appropriately modified ends of RNA molecules. Adapter-ligated RNA was reverse transcribed using a RNA primer complimentary to the 3'-adapter sequence and Superscript II Reverse Transcriptase (Invitrogen cat#18064-014). Adapter sequences were extended and index tags are added to the reverse transcribed cDNA by pcr (11 cycles). The pcr-amplified library is resolved on a 6%25 Novex TBE PAGE gel (Invitrogen cat#EC6265BOX) and a gel fragment representing the size range of adapter-modified small RNA cDNA was excised from the gel. Small RNA library molecules were eluted by soaking the crushed gel fragment

overnight in ultra-pure water at room temperature. Gel debris was removed from the eluate by centrifugal filtration of the sample across a 5 um filter. The concentration of the small RNA library was measured using the Invitrogen Qubit dsDNA HS Assay (Q32851) and an aliquot of the library was resolved on an Agilent 2200 Tape Station using a High Sensitivity D1K (cat# 5067-5363 and 5067-5364) assay to define the size distribution of the sequencing library. Libraries were adjusted to a concentration of approximately 5 nM and quantitative PCR was performed using the KapaBiosystems Kapa Library Quant Kit (cat# KK4824) to calculate the molarity of adapter ligated library molecules. The concentration was further adjusted following qPCR to prepare the library for Illumina sequence analysis.

Electrophysiology

Parasagittal cerebellar slices were made as described earlier in Hansen et al (3). In brief, age-matched WT and ATXN2-KO mice were anesthetized using isoflurane and decapitated in accordance with the protocol approved by the University of California Los Angeles Institutional Animal Care and Use Committee. The cerebellum was quickly dissected and placed in ice-cold extracellular solution (with composition in mM: 119 NaCl, 26 NaHCO3, 11 glucose, 2.5 KCl, 2.5 CaCl2, 1.3 MgCl2 and 1 NaH2PO4, pH 7.4 when gassed with 5% CO2 and 95% O2). Parasagittal cerebellar slices (285-µm thickness) were prepared on a Leica VT1000 vibratome (Leica, Germany) in ice-cold extracellular solution. Cerebellar slices were then incubated at 35 °C for 30 min and stored at room temperature until use. Temperature was set to 34.5+1°C (Model TC-344B, Warner Instruments) in the recording chamber and perfused cerebellar slices with extracellular solution at a rate of 2.8-3 ml/min. Purkinje cells were visualized with an

upright microscope (Leica) using 40x water immersion objective. Recordings were carried out with borosilicate glass electrodes (World Precision Instruments, USA) of 2–3 MΩ pulled on a P-1000 instrument (Sutter, USA) and filled with extracellular solution, the pipette potential was held at 0 mV and placed close to the axon hillock (soma/axon) of a Purkinje cell to measure action potential-associated capacitative current transients in voltage clamp mode for 2 minutes and typically 50 to 120 PCs were measured from three to six mice per genotype and the experimenter was kept blinded to the genotype. Currents were filtered at 4 kHz and sampled at 20 kHz using a Digidata 1440 and 700B amplifier (Axon Instruments). Spike detection was performed in pClamp 10 and further analysis Microsoft Excel or Igor software was used. Results are expressed as mean+SEM and figures are made in Igor program.

Funding

This work was supported by the National Institute of Health [XXXXX]: the National Library of Medicine Training Grant [5T15LM007124 to LP] and Richard A. Fay and Carol M. Fay Endowed Graduate Fellowship for the Department of Biomedical Informatics in Honor of Homer R. Warner, M.D., PhD. to LP.

Acknowledgements

Conflict of Interest

References

1. Pulst,S.-M., Nechiporuk,A., Nechiporuk,T., Gispert,S., Chen,X.-N., Lopes-Cendes,I., Pearlman,S., Starkman,S., Orozco-Diaz,G., Lunkes,A., *et al.* (1996)

Moderate expansion of a normally biallelic trinucleotide repeat in spinocerebellar ataxia type 2. *Nat. Genet.*, **14**, 269–276.

2. Matilla-Dueñas,A., Ashizawa,T., Brice,A., Magri,S., McFarland,K.N., Pandolfo,M., Pulst,S.M., Riess,O., Rubinsztein,D.C., Schmidt,J., *et al.* (2014) Consensus paper: pathological mechanisms underlying neurodegeneration in spinocerebellar ataxias. *Cerebellum Lond. Engl.*, **13**, 269–302.

3. Hansen,S.T., Meera,P., Otis,T.S. and Pulst,S.M. (2013) Changes in Purkinje cell firing and gene expression precede behavioral pathology in a mouse model of SCA2. *Hum. Mol. Genet.*, **22**, 271–283.

4. Dansithong,W., Paul,S., Figueroa,K.P., Rinehart,M.D., Wiest,S., Pflieger,L.T., Scoles,D.R. and Pulst,S.M. (2015) Ataxin-2 regulates RGS8 translation in a new BAC-SCA2 transgenic mouse model. *PLoS Genet.*, **11**, e1005182.

5. Damrath,E., Heck,M.V., Gispert,S., Azizov,M., Nowock,J., Seifried,C., Rüb,U., Walter,M. and Auburger,G. (2012) ATXN2-CAG42 Sequesters PABPC1 into Insolubility and Induces FBXW8 in Cerebellum of Old Ataxic Knock-In Mice. *PLOS Genet*, **8**, e1002920.

6. Kiehl,T.-R., Nechiporuk,A., Figueroa,K.P., Keating,M.T., Huynh,D.P. and Pulst,S.-M. (2006) Generation and characterization of Sca2 (ataxin-2) knockout mice. *Biochem. Biophys. Res. Commun.*, **339**, 17–24.

7. Lastres-Becker,I., Brodesser,S., Lütjohann,D., Azizov,M., Buchmann,J., Hintermann,E., Sandhoff,K., Schürmann,A., Nowock,J. and Auburger,G. (2008) Insulin receptor and lipid metabolism pathology in ataxin-2 knock-out mice. *Hum. Mol. Genet.*, **17**, 1465–1481.

8. Somvanshi,P.R. and Venkatesh,K.V. (2014) A conceptual review on systems biology in health and diseases: from biological networks to modern therapeutics. *Syst. Synth. Biol.*, **8**, 99–116.

9. Keifer,J. and Summers,C.H. (2016) Putting the 'Biology' Back into 'Neurobiology': The Strength of Diversity in Animal Model Systems for Neuroscience Research. *Front. Syst. Neurosci.*, **10**.

10. Huang,D.W., Sherman,B.T. and Lempicki,R.A. (2008) Systematic and integrative analysis of large gene lists using DAVID bioinformatics resources. *Nat. Protoc.*, **4**, 44–57.

11. Ashburner,M., Ball,C.A., Blake,J.A., Botstein,D., Butler,H., Cherry,J.M., Davis,A.P., Dolinski,K., Dwight,S.S., Eppig,J.T., *et al.* (2000) Gene Ontology: tool for the unification of biology. *Nat. Genet.*, **25**, 25–29.

12. Rong,Y., Wang,T. and Morgan,J.I. (2004) Identification of candidate Purkinje cell-specific markers by gene expression profiling in wild-type and pcd3J mice. *Mol. Brain Res.*, **132**, 128–145.

13. Larvie,M., Shoup,T., Chang,W.-C., Chigweshe,L., Hartshorn,K., White,M.R., Stahl,G.L., Elmaleh,D.R., Takahashi,K., Larvie,M., *et al.* (2012) Mannose-Binding Lectin Binds to Amyloid β Protein and Modulates Inflammation, Mannose-Binding Lectin Binds to Amyloid β Protein and Modulates Inflammation. *BioMed Res. Int. BioMed Res. Int.*, **2012**, **2012**, e929803.

14. Langfelder,P. and Horvath,S. (2008) WGCNA: an R package for weighted correlation network analysis. *BMC Bioinformatics*, **9**, 559.

15. Zhang,B. and Horvath,S. (2005) A general framework for weighted gene co-expression network analysis. *Stat. Appl. Genet. Mol. Biol.*, **4**, Article17.

16. Langfelder,P., Mischel,P.S. and Horvath,S. (2013) When Is Hub Gene Selection Better than Standard Meta-Analysis? *PLoS ONE*, **8**, e61505.

17. Langfelder,P. and Horvath,S. (2007) Eigengene networks for studying the relationships between co-expression modules. *BMC Syst. Biol.*, **1**, 54.

18. Stepanov,G.A., Filippova,J.A., Komissarov,A.B., Kuligina,E.V., Richter,V.A., Semenov,D.V., Stepanov,G.A., Filippova,J.A., Komissarov,A.B., Kuligina,E.V., *et al.* (2015) Regulatory Role of Small Nucleolar RNAs in Human Diseases, Regulatory Role of Small Nucleolar RNAs in Human Diseases. *BioMed Res. Int. BioMed Res. Int.*, **2015**, **2015**, e206849.

19. Papadopoulou,A.S., Serneels,L., Achsel,T., Mandemakers,W., Callaerts-Vegh,Z., Dooley,J., Lau,P., Ayoubi,T., Radaelli,E., Spinazzi,M., *et al.* (2015) Deficiency of the miR-29a/b-1 cluster leads to ataxic features and cerebellar alterations in mice. *Neurobiol. Dis.*, **73**, 275–288.

20. Ingram,M., Wozniak,E.A.L., Duvick,L., Yang,R., Bergmann,P., Carson,R., O'Callaghan,B., Zoghbi,H.Y., Henzler,C. and Orr,H.T. (2016) Cerebellar Transcriptome Profiles of ATXN1 Transgenic Mice Reveal SCA1 Disease Progression and Protection Pathways. *Neuron*, **89**, 1194–1207.

21. Luthi-Carter,R., Strand,A.D., Hanson,S.A., Kooperberg,C., Schilling,G., La Spada,A.R., Merry,D.E., Young,A.B., Ross,C.A., Borchelt,D.R., *et al.* (2002) Polyglutamine and transcription: gene expression changes shared by DRPLA and Huntington's disease mouse models reveal context-independent effects. *Hum. Mol. Genet.*, **11**, 1927–1937.

22. Friedrich,B., Euler,P., Ziegler,R., Kuhn,A., Landwehrmeyer,B.G., Luthi-Carter,R., Weiller,C., Hellwig,S. and Zucker,B. (2012) Comparative analyses of Purkinje cell gene expression profiles reveal shared molecular abnormalities in models of different polyglutamine diseases. *Brain Res.*, **1481**, 37–48.

23. Evert,B.O., Vogt,I.R., Vieira-Saecker,A.M., Ozimek,L., de Vos,R.A.I., Brunt,E.R.P., Klockgether,T. and Wüllner,U. (2003) Gene Expression Profiling in Ataxin-3 Expressing Cell Lines Reveals Distinct Effects of Normal and Mutant Ataxin-3. *J. Neuropathol. Exp. Neurol.*, **62**, 1006–1018.

24. Lucas,E.K., Reid,C.S., McMeekin,L.J., Dougherty,S.E., Floyd,C.L. and Cowell,R.M. (2015) Cerebellar transcriptional alterations with Purkinje cell dysfunction and loss in mice lacking PGC-1Î±. *Front. Cell. Neurosci.*, **8**.

25. Yoo,S.Y., Pennesi,M.E., Weeber,E.J., Xu,B., Atkinson,R., Chen,S., Armstrong,D.L., Wu,S.M., Sweatt,J.D. and Zoghbi,H.Y. (2003) SCA7 knockin mice model human SCA7 and reveal gradual accumulation of mutant ataxin-7 in neurons and abnormalities in short-term plasticity. *Neuron*, **37**, 383–401.

26. Watase,K., Barrett,C.F., Miyazaki,T., Ishiguro,T., Ishikawa,K., Hu,Y., Unno,T., Sun,Y., Kasai,S., Watanabe,M., *et al.* (2008) Spinocerebellar ataxia type 6 knockin mice develop a progressive neuronal dysfunction with age-dependent accumulation of mutant CaV2.1 channels. *Proc. Natl. Acad. Sci. U. S. A.*, **105**, 11987–11992.

27. Crespo-Barreto,J., Fryer,J.D., Shaw,C.A., Orr,H.T. and Zoghbi,H.Y. (2010) Partial Loss of Ataxin-1 Function Contributes to Transcriptional Dysregulation in Spinocerebellar Ataxia Type 1 Pathogenesis. *PLoS Genet.*, **6**.

28. Miller,J.A., Woltjer,R.L., Goodenbour,J.M., Horvath,S. and Geschwind,D.H. (2013) Genes and pathways underlying regional and cell type changes in Alzheimer's disease. *Genome Med.*, **5**, 48.

29. Fogel,B.L., Cho,E., Wahnich,A., Gao,F., Becherel,O.J., Wang,X., Fike,F., Chen,L., Criscuolo,C., De Michele,G., *et al.* (2014) Mutation of senataxin alters disease-specific transcriptional networks in patients with ataxia with oculomotor apraxia type 2. *Hum. Mol. Genet.*, **23**, 4758–4769.

30. Bettencourt,C., Forabosco,P., Wiethoff,S., Heidari,M., Johnstone,D.M., Botía,J.A., Collingwood,J.F., Hardy,J., Milward,E.A., Ryten,M., *et al.* (2016) Gene co-expression networks shed light into diseases of brain iron accumulation. *Neurobiol. Dis.*, **87**, 59–68.

31. Provenzano,G., Corradi,Z., Monsorno,K., Fedrizzi,T., Ricceri,L., Scattoni,M.L. and Bozzi,Y. (2016) Comparative Gene Expression Analysis of Two Mouse Models of Autism: Transcriptome Profiling of the BTBR and En2 (-/-) Hippocampus. *Front. Neurosci.*, **10**, 396.

32. Maciotta,S., Meregalli,M. and Torrente,Y. (2013) The involvement of microRNAs in neurodegenerative diseases. *Front. Cell. Neurosci.*, **7**, 265.

Figure Legends

Figure 1. Overview of gene expression profiles of cerebellar tissue of ATXN2-Q127 mice at three time points. **(A)** Number of shared and specific differentially expressed genes across three time points. **(B)** Number of up- (red) and down- (green) differentially regulated genes in cerebella of ATXN2-Q127 mice compared to WT mice at each time point.

Figure 2. Gene co-expression modules. (A) Identification of gene co-expression modules in ATXN2-Q127 mice with age matches controls. Branches of the cluster dendrogram gave rise to 16 color-coded modules when modules with 10% similarity were merged. **(B)** Gene significance per module as determined by enrichment for genes

with high differential expression between ATXN2-Q127 and controls. The black, darkgrey, darkred and midnightblue modules were the only significant modules as determined by P-value less than 0.05.

Figure 3. Co-expression network of relevant modules. Network representation of (A) black (B) darkgrey (C) darkred and (D) midnightblue modules. Visual representation generated using VisANT (REF). Given TOM cut-offs, not all genes corresponding to each module are represented.

Figure 4. Validation of key genes. Needs updated with p-values.

Figure 5. Comparison of differentially expressed genes between mouse models. Venn diagrams of differentially expressed genes (Het = heterozygous for *Atxn2*, TG=ATXN2-Q127 and KO= Sca2(-/-)) at 1 day and 60 day/6 week time points models.

Figure 6. Knockout of the *Atxn2* gene in mice did not change Purkinje cell firing in the acute cerebellar slice Purkinje cell firing frequency distribution plot determined by extracellular recordings in acute cerebellar slices from *Atxn2* knockout mice ages 4, 12, and 24 weeks of WT (A) and SCO2-KO (B). Alexa dye filled Purkinje Neuron in WT (C) and SCA2-KO (D) in 24 wks old mice.

Tables

Table 1. Top 10 hub genes as ranked by intramodule connectivity for each of the gene significant modules

Black	Darkgrey	Darkred	Midnightblue
Smarca4	*Cep76*	*Cyth3*	*Gabbr2*
Rusc2	*Calb1*	*Dgkz*	*Dagla*
Pcdhga9	*Stk17b*	*Gabbr1*	*Doc2b*
Ankrd11	*Pcp4*	*Sbk1*	*Atp2a2*

Lmtk2	*Dpp10*	*Fam21*	*Prkcg*
Sptb	*Kcnab1*	*Icmt*	*Atp2b2*
Dnm1	*Ppp1r17*	*Rnf19b*	*Mprip*
Cep170b	*Cep72*	*Garnl3*	*Cacna1g*
Phf2	*Gm13944*	*Aldoc*	*Arhgap26*
Agap1	*Arhgef33*	*Homer3*	*Shank2*

Table 2. Differentially expressed miRNA and snoRNA at 3 weeks.

Gene Name	Gene Biotype	Location	Fold Change
snord115	snoRNA	chr7:59389819-59389898	23.85819509
snord115	snoRNA	chr7:59424923-59425002	15.60283195
snord115	snoRNA	chr7:59353282-59353361	9.942481689
snord115	snoRNA	chr7:59436148-59436227	3.796002651
snord115	snoRNA	chr7:59423054-59423133	3.396808767
Mir199b	miRNA	chr2:32318459-32318569	2.462080615
Mir203	miRNA	chr12:112130879-112130955	2.628937784
Mir499	miRNA	chr2:155622879-155622958	2.157976269
Mir1197	miRNA	chr12:109712316-109712436	2.593526301
Mir142	miRNA	chr11:87756863-87756927	2.602084838
Mir1193	miRNA	chr12:109715670-109715791	2.13206881
snord116	snoRNA	chr7:59681054-59681148	2.592665348
Mir144	miRNA	chr11:78073004-78073070	2.618330112
Mir653	miRNA	chr6:3721300-3721385	2.47143335
Mir544	miRNA	chr12:109729324-109729402	2.165544772
Mir208a	miRNA	chr14:54949059-54949142	2.038487344
Gm24895	snoRNA	chr12:109646128-109646202	0.47198241
Mir669l	miRNA	chr2:10468970-10469068	1.934303262
Gm22620	snoRNA	chr9:15315188-15315321	1.850769206
Mir133b	miRNA	chr1:20682768-20682887	1.909787341
Mir214	miRNA	chr1:162223367-162223477	2.038867469
Mir3059	miRNA	chr10:101772691-101772772	2.309486319
Mir483	miRNA	chr7:142654923-142654996	1.847473922
Mir708	miRNA	chr7:96249423-96249532	2.203793429

Figures

Figure 1

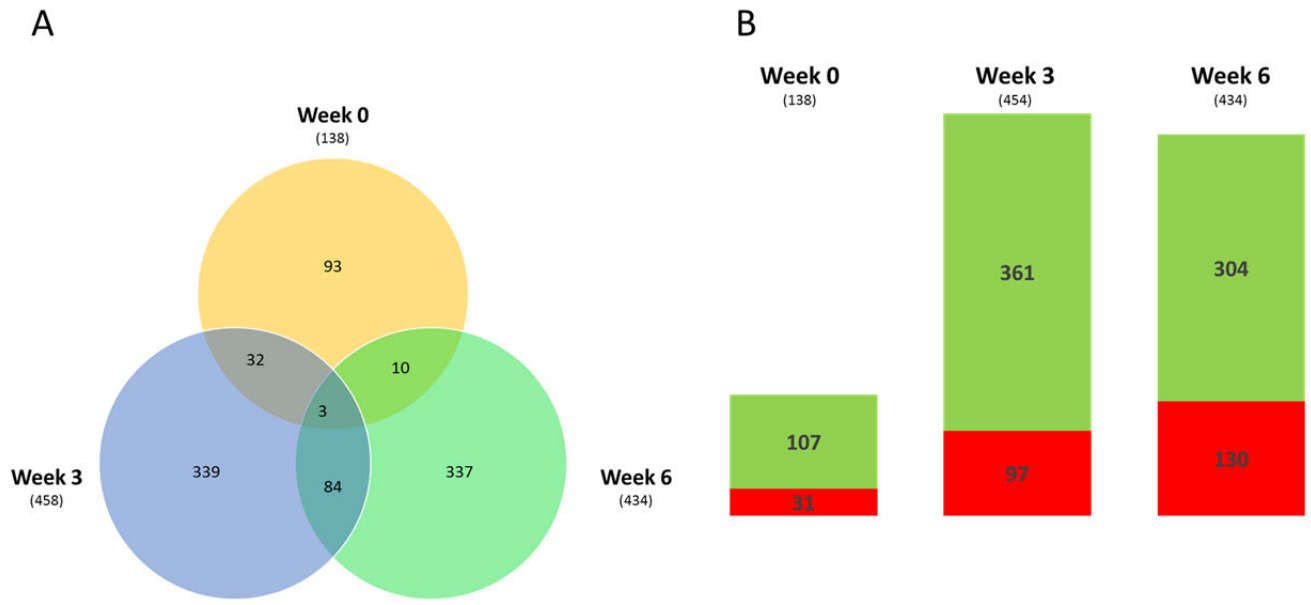
A
Week 0
(138)
93
32
10
3
Week 3
(458)
339
84
337
Week 6
(434)
B
Week 0
(138)
Week 3
(454)
Week 6
(434)
107
31
361
97
304
130

Figure 2

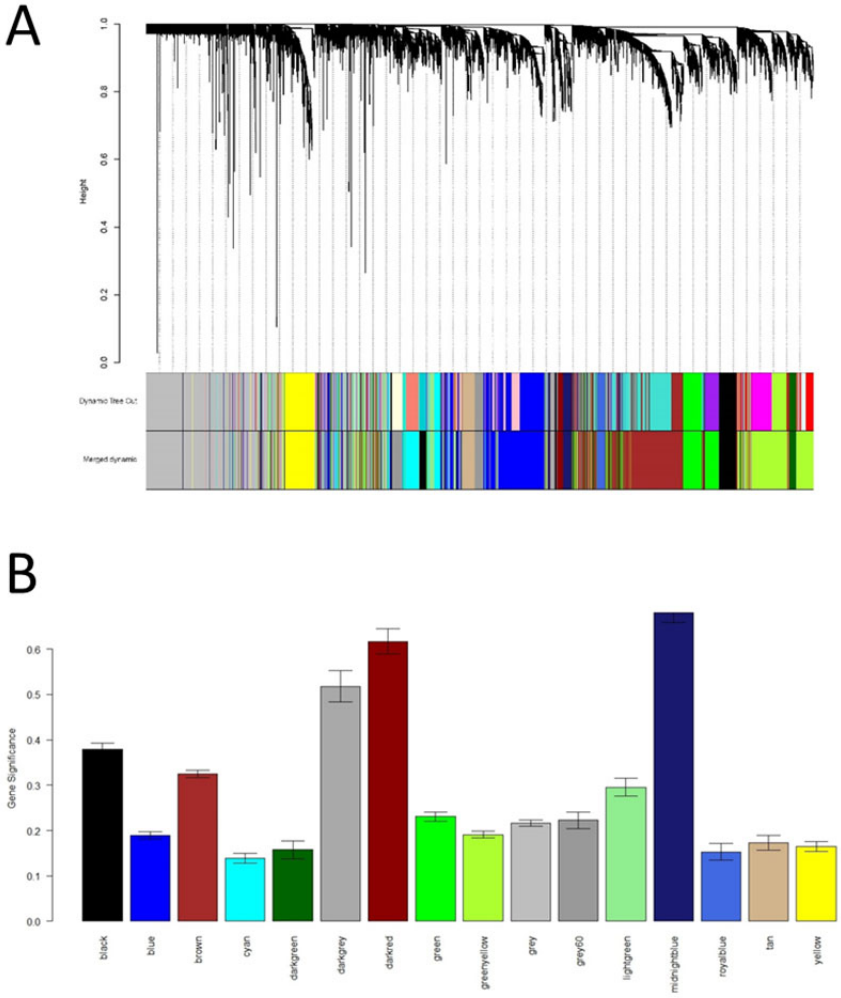
A
Height
1.0
0.8
0.6
0.4
0.2
0.0
Dynamic Tree Cut
Merged dynamic
B
Gene Significance
0.6
0.5
0.4
0.3
0.2
0.1
0.0
black
blue
brown
cyan
darkgreen
darkgrey
darkred
green
greenyellow
grey
grey60
lightgreen
midnightblue
royalblue
tan
yellow

Figure 3

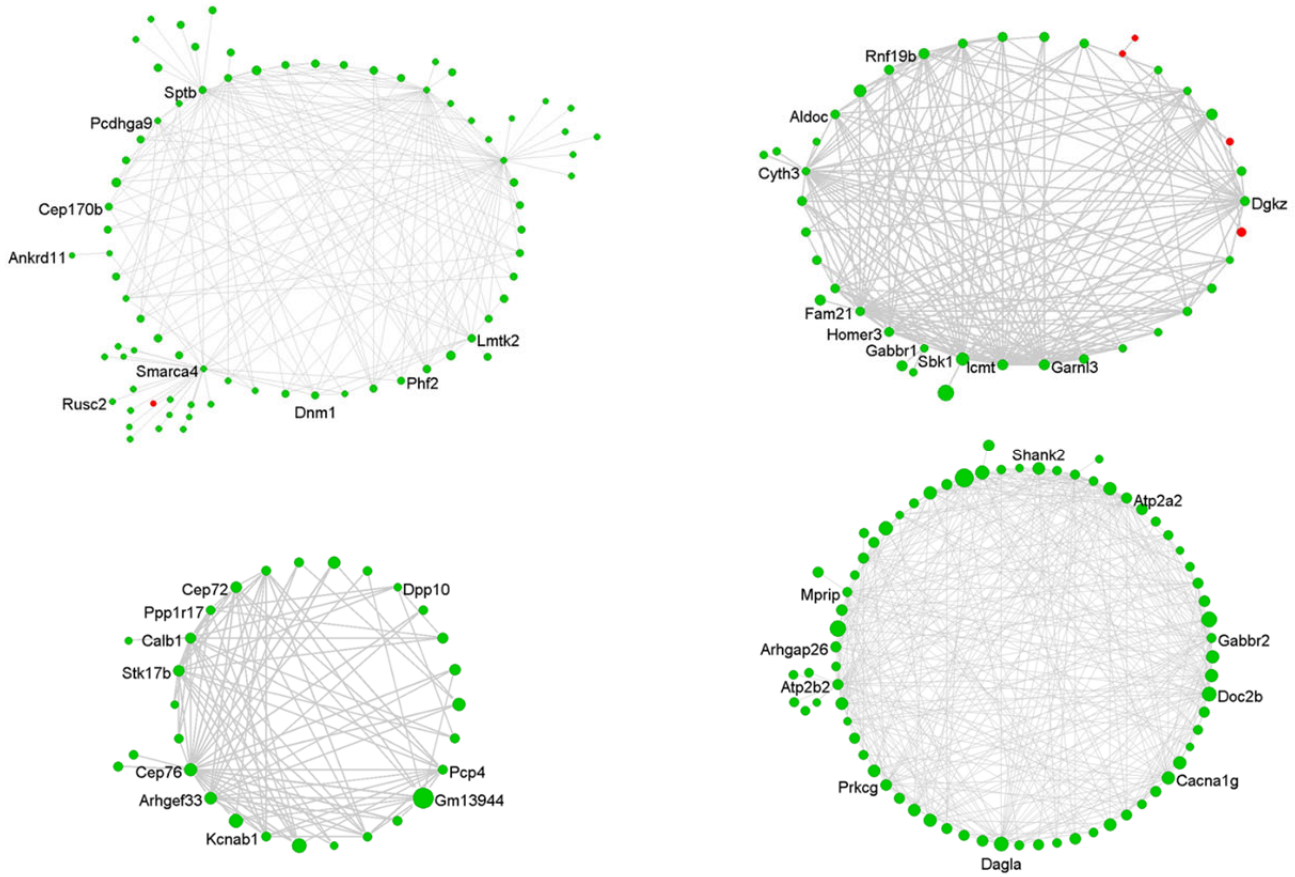
Sptb
Pcdhga9
Cep170b
Ankrd11
Smarca4
Rusc2
Dnm1
Phf2
Lmtk2
Rnf19b
Aldoc
Cyth3
Dgkz
Fam21
Homer3
Gabbr1
Sbk1
Icmt
Garnl3
Cep72
Ppp1r17
Calb1
Stk17b
Cep76
Arhgef33
Kcnab1
Dpp10
Pcp4
Gm13944
Shank2
Atp2a2
Mprip
Arhgap26
Atp2b2
Prkcg
Dagla
Gabbr2
Doc2b
Cacna1g

Figure 4

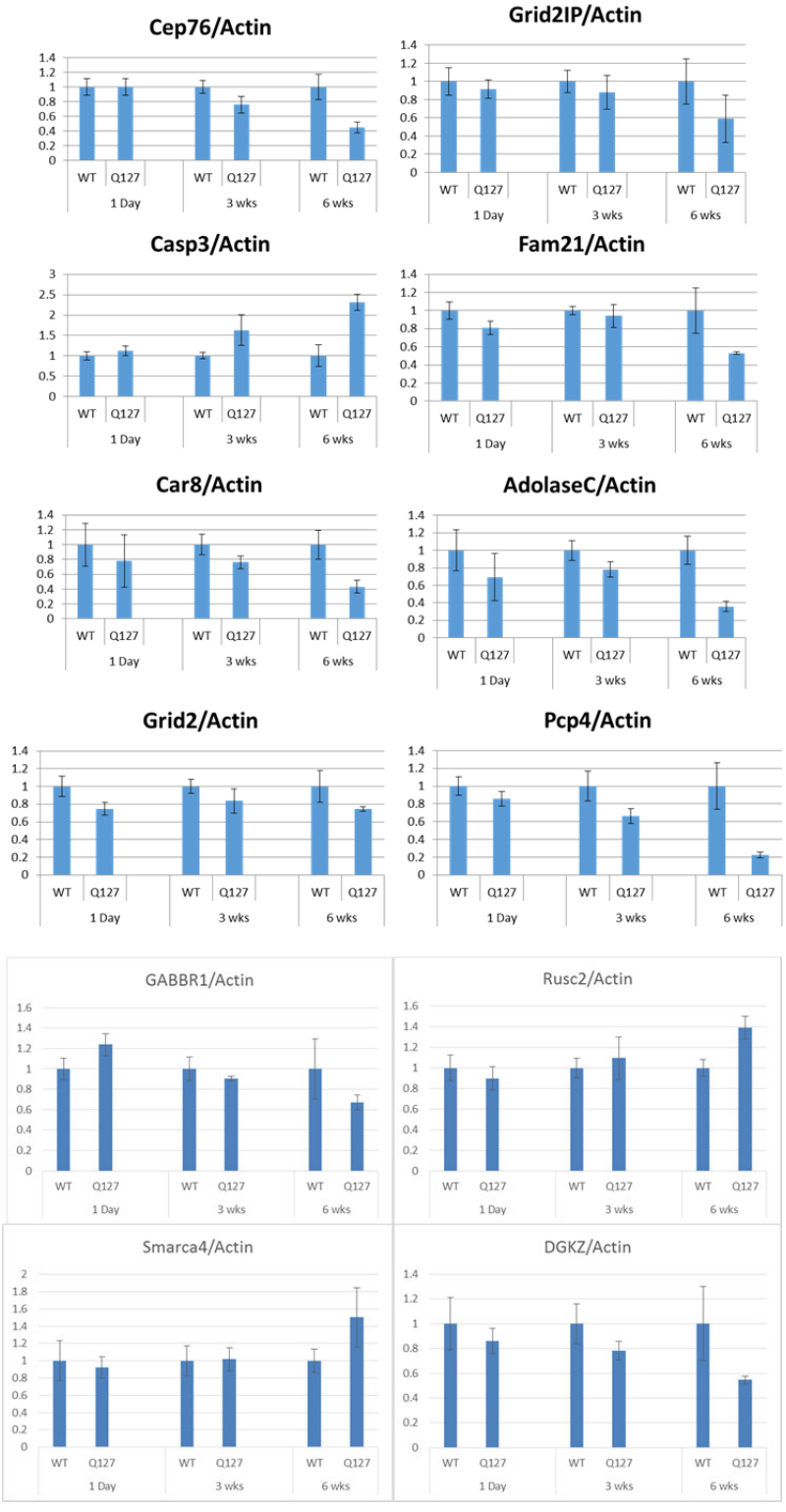
Cep76/Actin
Grid2IP/Actin
Casp3/Actin
Fam21/Actin
Car8/Actin
AdolaseC/Actin
Grid2/Actin
Pcp4/Actin
GABBR1/Actin
Rusc2/Actin
Smarca4/Actin
DGKZ/Actin
WT
Q127
1 Day
3 wks
6 wks

Figure 5

Figure 6

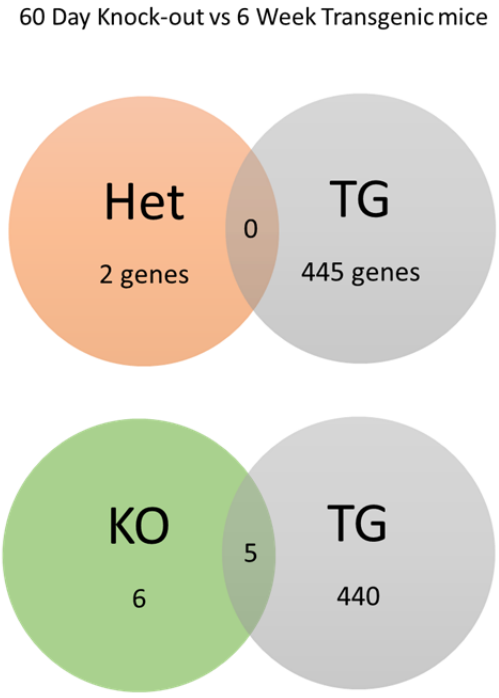
60 Day Knock-out vs 6 Week Transgenic mice
Het
2 genes
0
TG
445 genes
KO
6
5
TG
440

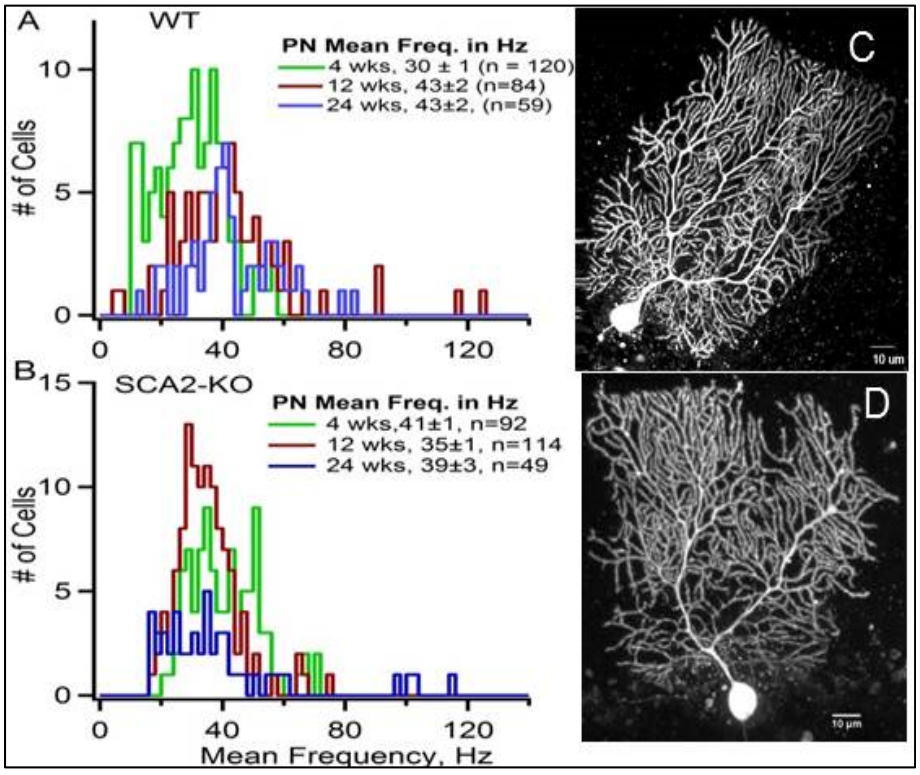
A
WT
PN Mean Freq. in Hz
4 wks, 30 ± 1 (n = 120)
12 wks, 43±2 (n=84)
24 wks, 43±2, (n=59)
# of Cells
10
5
0
0
40
80
120
C
10 um
B
SCA2-KO
PN Mean Freq. in Hz
4 wks,41±1, n=92
12 wks, 35±1, n=114
24 wks, 39±3, n=49
# of Cells
15
10
5
0
0
40
80
120
Mean Frequency, Hz
D
10 µm